



Original Articles

Blocking MARCO⁺ tumor-associated macrophages improves anti-PD-L1 therapy of hepatocellular carcinoma by promoting the activation of STING-IFN type I pathway



Limin Ding ^{a,b,c,d,1}, Junjie Qian ^{a,b,c,d,1}, Xizhi Yu ^{a,b,c,d,1}, Qinchuan Wu ^{a,b,c,d}, Jing Mao ^{a,b,c,d}, Xi Liu ^{a,b,c,d}, Yubo Wang ^{a,b,c,d}, Danjing Guo ^{b,c,d}, Rong Su ^{b,c,d}, Haiyang Xie ^{b,c,d}, Shengyong Yin ^{b,c,d}, Lin Zhou ^{b,c,d,**}, ShuSen Zheng ^{a,b,c,d,*}

^a Division of Hepatobiliary and Pancreatic Surgery, Department of Surgery, The First Affiliated Hospital, Zhejiang University School of Medicine, Hangzhou, 310003, China

^b NHC Key Laboratory of Combined Multi-organ Transplantation, Hangzhou, 310003, China

^c Key Laboratory of the Diagnosis and Treatment of Organ Transplantation, Research Unit of Collaborative Diagnosis and Treatment for Hepatobiliary and Pancreatic Cancer, Chinese Academy of Medical Sciences (2019RU019), Hangzhou, 310003, China

^d Key Laboratory of Organ Transplantation, Research Center for Diagnosis and Treatment of Hepatobiliary Diseases, Zhejiang Province, Hangzhou, 310003, China

ARTICLE INFO

Keywords:

Hepatocellular carcinoma
MARCO
Tumor-associated macrophages
IFN- β
PD-L1

ABSTRACT

The PD-L1/PD-1 axis is a classic immunotherapy target. However, anti-PD-L1/PD-1 therapy alone can not achieve satisfactory results in solid tumors, especially liver cancer. Among the several factors involved in tumor anti-PD-L1/PD-1 treatment resistance, tumor-associated macrophages (TAMs) have attracted attention because of their immunosuppressive ability. TAMs with a macrophage receptor with a collagenous structure (MARCO) are a macrophage subset group with strong immunosuppressive abilities. Clinical specimens and animal experiments revealed a negative correlation between MARCO⁺ TAMs and patient prognosis with liver cancer. Transcriptional data and *in vitro* and *in vivo* experiments revealed that MARCO⁺ TAM immunosuppressive ability was related to secretion. MARCO suppressed IFN- β secretion from TAMs, reducing antigen presentation molecule expression, infiltration, and CD8⁺T cell dysfunction, thus producing an immunosuppressive microenvironment in liver cancer. MARCO can promote dying tumor cell clearance by macrophages, reducing tumor-derived cGAMP and ATP accumulation in the tumor microenvironment and inhibiting sting-IFN- β pathway activation mediated by P2X7R in MARCO⁺ TAMs. Animal experiments revealed that the MARCO and PD-L1 monoclonal antibody combination could significantly inhibit liver cancer growth. Conclusively, targeting MARCO⁺ TAMs can significantly improve anti-PD-L1 resistance in liver cancer, making it a potential novel immune target for liver cancer therapy.

1. Introduction

Worldwide, hepatocellular carcinoma (HCC) is one of the leading cause of cancer related deaths [1]. Immune checkpoint inhibition therapy, which involves inhibiting programmed cell death protein-1 (PD-1) and its ligand (PD-L1) to increase T cell tumor-killing function, has emerged as a novel treatment for liver cancer [2]. However, patients with liver cancer have a low response rate to treatment, and some

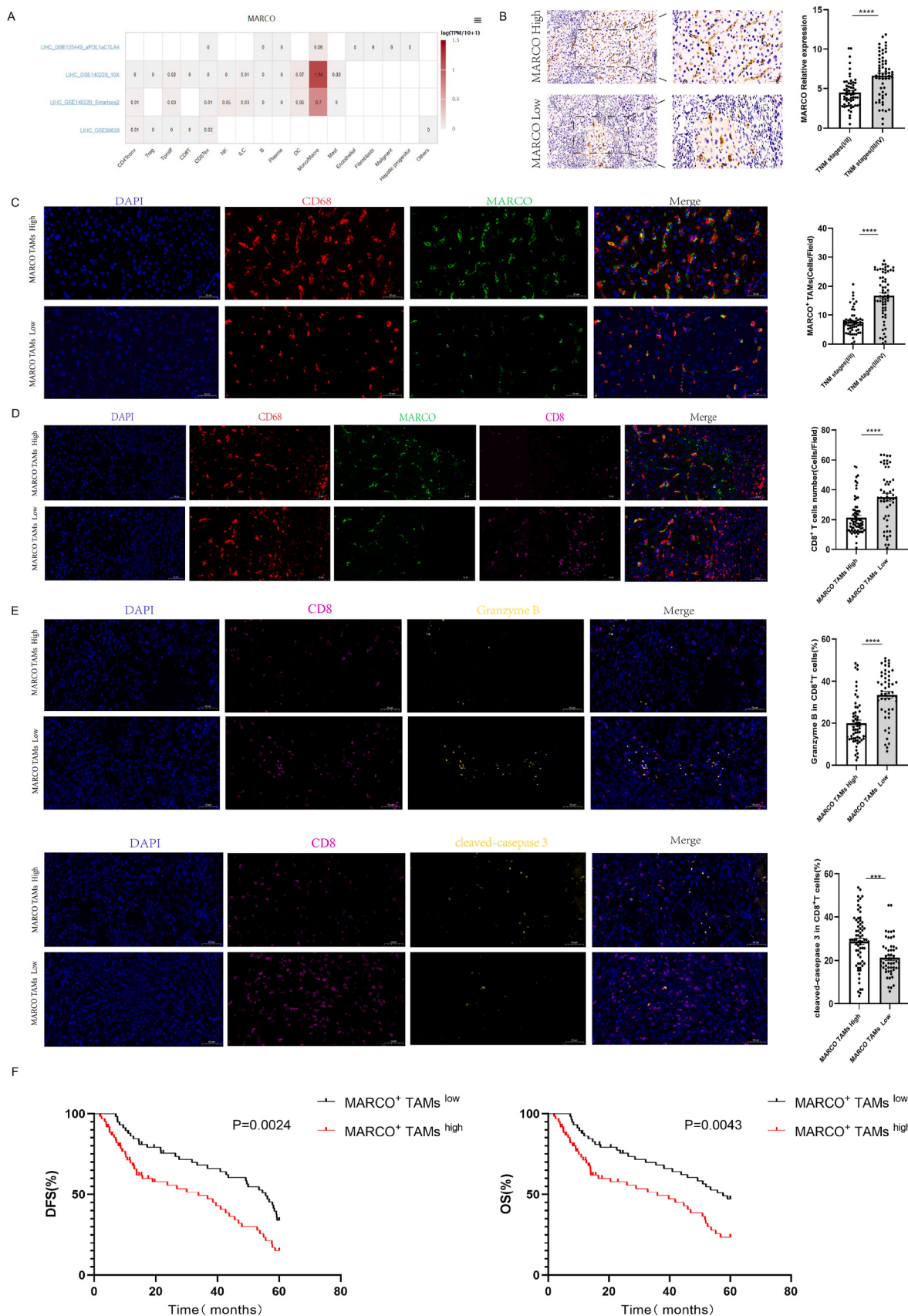
patients who originally responded to treatment develop drug resistance [3,4]. Many causal factors influence the therapeutic effect of anti-PD-L1/PD-1, including low-level infiltration and dysfunction of CD8⁺T cells in the tumor [5,6]. In addition, an immunosuppressive tumor microenvironment is one of the primary causes of the low response rate of tumors to immunotherapy [3]. Tumor-associated macrophages (TAMs), the most numerous immune cells in the tumor microenvironment of liver cancer, play a critical role in tumor incidence

* Corresponding author. Division of Hepatobiliary and Pancreatic Surgery, Department of Surgery, The First Affiliated Hospital, Zhejiang University School of Medicine, Hangzhou, 310003, China.

** Corresponding author. NHC Key Laboratory of Combined Multi-organ Transplantation, Hangzhou, 310003, China.

E-mail addresses: zhoul99@zju.edu.cn (L. Zhou), shusenzheng@zju.edu.cn (S. Zheng).

¹ These authors contributed equally to this work.



(caption on next page)

Fig. 1. MARCO is mainly expressed on the macrophage surface in the HCC microenvironment and is negatively correlated with patient prognosis.

- (A) Different immune cells expression patterns of MARCO in four single-cell sequences of LIHC (hepatocellular carcinoma).
- (B) Immunohistochemical staining of MARCO in hepatocellular carcinoma (left panel, magnification of $\times 200$, right panel, magnification of $\times 400$). According to the immunohistochemical staining score and clinical data, the relationship between MARCO relative expression in tumor tissue and the HCC TNM stage was analyzed. Data are expressed as mean \pm SEM ($n = 121$).
- (C) Representative images of MARCO (green), CD68 (red), and DAPI (blue) immunofluorescence staining in HCC tissues at $\times 400$ magnification. According to the average number of MARCO⁺ TAMs in 10 random fields of HCC tissues and clinical case data, the relationship between MARCO⁺ TAM relative expression in tumor tissues and the HCC TNM stage was analyzed. Data are expressed as mean \pm SEM ($n = 121$).
- (D) Co-staining with MARCO (green), CD68 (red), DAPI (blue), and CD8 (rose red) in HCC tissues with high MARCO⁺TAMs (number ≥ 6 per game) or low CD68 (number per game < 6) at magnification of $\times 400$, comparing the average number of CD8⁺ T cells in 10 random fields in HCC tissues with high MARCO⁺ TAMs ($n = 69$) and low MARCO⁺ TAMs ($n = 52$). Data are expressed as mean \pm SEM.
- (E) CD8 (rose red), cleaved-caspase 3 (orange), and Granzyme B (orange) were stained in HCC tissues with high or low MARCO⁺TAMs at a magnification of $\times 400$. The percentages of Granzyme B (upper) and cleaved-caspase 3 (lower) of CD8⁺ T cells in 10 random fields in HCC tissues with high ($n = 69$) and low MARCO⁺ TAMs ($n = 52$) were compared. Data are expressed as mean \pm SEM.
- (F) MARCO⁺TAM survival analysis: The total survival and disease-free survival curves of the high MARCO⁺TAMs group ($n = 69$) and low MARCO⁺TAMs group ($n = 52$) were compared. * $p < 0.05$; ** $p < 0.01$; *** $p < 0.001$; **** $p < 0.0001$. Abbreviations: DAPI 4',6-diamidino-2-phenylindole; C-Cas-3, cleaved caspase-3.

and progression [7]. TAMs are a highly differentiated cell population. TAMs originate from embryonic macrophages, neonatal monocytes, and adult monocyte-derived macrophages [8]. TAMs are functionally classified as M1 with immune promotion, M2 with immunosuppressive effect, and macrophage subsets with varying degrees of anti-inflammatory and pro-inflammatory effects [9]. TAMs can also promote tumor metastasis and angiogenesis while inhibiting antitumor immunity [10]. Recent studies have revealed that TAMs can enhance or inhibit the antitumor activity of chemotherapeutic drugs, radiotherapy, anti-angiogenic drugs, and immune checkpoint inhibitors. This discrepancy is strongly linked to heterogeneity [11].

The collagen-like structure macrophage receptor (MARCO) is a class A scavenger receptor family member found mostly on the surfaces of macrophages and dendritic cells [12,13]. Macrophages with higher MARCO expression have a stronger affinity to bind pathogens and phagocytose low-density lipoproteins [12]. In the alveoli, the major receptor for silica binding and phagocytosis is MARCO expressed on the surface of macrophages; therefore, macrophages with high MARCO expression play a key role in silica-induced pulmonary fibrosis and silicosis [14,15]. It has been shown that MARCO⁺ microglia in the central nervous system bind to alpha-amyloid proteins and are responsible for causing Alzheimer's disease to develop and progress [16]. Furthermore, MARCO, a scavenger receptor, improves the uptake of low-density lipoproteins by macrophages in the cardiovascular system, boosting cholesterol accumulation in foam cells and exacerbating the formation of atherosclerotic plaques [17]. In recent years, MARCO⁺ macrophages have been linked to forming an immunosuppressive tumor microenvironment. They are highly related to the poor prognosis of melanoma, breast, colon, lung, pancreatic, and prostate cancer [18–21]. However, the mechanism by which MARCO⁺TAMs regulate tumor microenvironment is unclear, and its role in the incidence and progression of HCC as a solid tumor rich in macrophages has received little attention.

P2X7R is a ATP-gated channel for transporting small molecules. When damaged or dying cells are left uncleared, apoptotic cells can develop to necrotic cells and release intracellular constituents, including cGAMP and ATP [22]. In this case, a high level of extracellular ATP (eATP) can potentially open the ATP-gated P2X7R channel and allow the direct passage of nanometer-sized molecules, including cGAMP. This can activate intracellular stimulators of interferon genes (STING) pathway in macrophage, leading to boosted expression of downstream type I interferon [23]. However, whether P2X7R-STING-type I interferon pathway contributed to MARCO⁺ macrophages-regulated tumor immune microenvironment remains enigmatic.

In this study, we found a significant negative correlation between MARCO⁺TAMs in the tumor microenvironment and the prognosis of patients with liver cancer. Owing to the fact that MARCO⁺TAM has a strong phagocytic ability, it can quickly remove dying tumor cells from the tumor microenvironment and minimize the accumulation of tumor-

derived cyclic guanosine monophosphate–adenosine monophosphate (cGAMP) and ATP. Extracellular ATP deficiency inhibits P2X7R-mediated cGAMP transport on TAM surfaces. It also inhibits the activation of intracellular stimulators of interferon genes (STING) pathways, causing a decrease in type I interferon secretion in macrophages. Blocking the phagocytic ability of MARCO using specific neutralizing antibodies can significantly increase the level of type I interferon secretion by TAMs, boost their antigen presentation ability, increase CD8⁺ T cell infiltration in the tumor microenvironment, enhance their function, and effectively improve the antitumor effect of anti-PD-L1 therapy.

2. Materials and methods

2.1. Clinical samples

A total of 121 tissue samples were obtained from our hospital's patients who underwent curative resection for HCC between 2014 and 2017. Immunohistochemistry (IHC), immunofluorescence, and survival analyses were performed on the tissues. This study was approved by our hospital's Ethics Committee(20230322). Table S1 summarizes the clinical data of all patients.

2.2. Cell culture and transfection

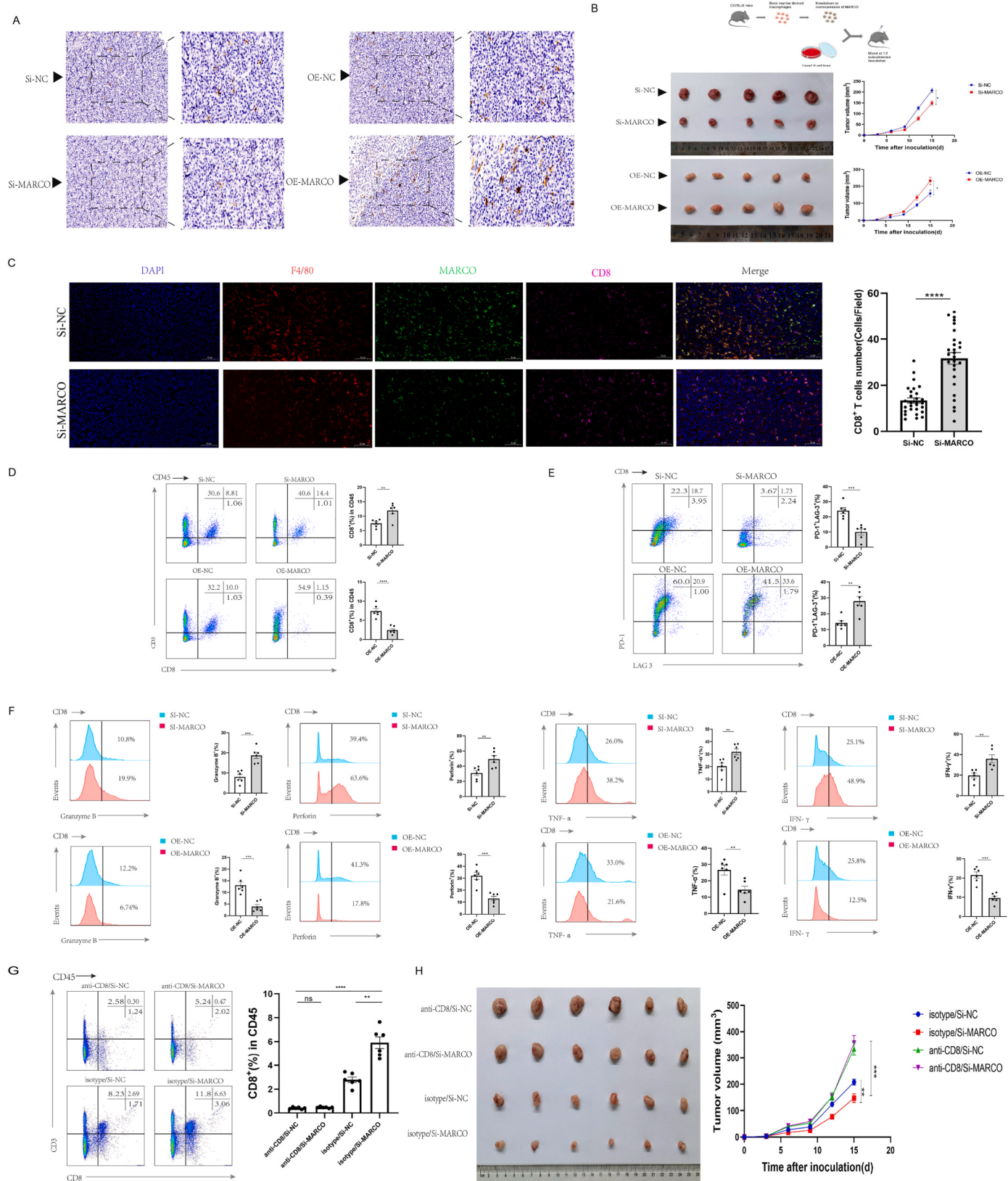
Supplementary materials demonstrate cell culture and transfection methods.

2.3. Establishment of mouse tumor model and treatment

Animal experiments were approved by our hospital Animal Care Committee according to the guidelines of the Institutional Animal Care and Use Committee.In this study, C57BL/6J, C57BL/6J OT-1, C57BL/6J STING1^{-/-}mice(male, 6–8 weeks old) were mainly used. Experimental mice were fed at the SPF animal center. A detailed description of the drug treatments is given in the supplementary materials following the establishment of the mouse tumor model.

2.4. Flow cytometry and single-cell suspension preparation

On the specified day, the mice were euthanized, and the orthotopic or subcutaneous tumor was collected. OptiPrep Density Gradient Medium was used to extract mononuclear cells from a single-cell culture. After antibody incubation, multicolor flow cytometry was used to detect CD8⁺ T cells enriched with magnetic beads (551516; BD Biosciences). Leukocyte Activation Cocktail (550583, BD Pharmingen, San Diego, CA, USA) was used to stimulate CD8⁺ T cells for 5 h to assess cytotoxic activity. Supplementary Materials shows the specific staining steps and antibodies used.



(caption on next page)

Fig. 2. MARCO⁺ TAMs mediate hepatocellular carcinoma progression by inhibiting CD8⁺T cell infiltration and inducing its dysfunction. (A) MARCO immunohistochemical staining of subcutaneous tumor tissues in MARCO knockdown (left) and overexpression (right) groups. (B) A tumor model was established by subcutaneous inoculating Hepa1-6 cells mixed with macrophages (at a 2:1 ratio) into C57BL/6 mice. As shown in the schematic diagram (above is the knockdown group, denoted Si-NC and Si-MARCO, respectively; below is the overexpressed group, denoted OE-NC and OE-MARCO, respectively), tumor growth was monitored regularly, and the data of tumor volume was represented as mean ± SEM ($n = 6$ in each group). (C) Representative images of immunofluorescence staining in subcutaneous tumor tissues of the Si-NC ($n = 28$) and Si-MARCO groups ($n = 27$), with staining of CD68 (red), MARCO (green), DAPI (blue), and CD8 (rose red). CD8⁺ T cell average number in 10 random plots at $\times 400$ ratio was expressed as mean ± SEM. (D) CD8⁺ T cell ratio to CD45⁺ in MARCO knockdown and overexpression groups was expressed as mean ± SEM ($n = 6$ in each group). (E) CD8⁺ T cells were isolated and enriched from subcutaneous tumor tissues of MARCO knockdown and overexpression groups. Flow cytometry was used to analyze the exhausted status of CD8⁺ T cells (PD-1⁺ and LAG-3⁺ labeling). Data are expressed as mean ± SEM ($n = 6$ in each group). (F) CD8⁺ T cells were isolated and enriched from subcutaneous tumor tissues of MARCO knockdown and overexpression groups, and CD8⁺ T cell cytotoxic function (granzyme B⁺, perforin⁺, TNF- α ⁺, and IFN- γ ⁺ labeling) was analyzed using flow cytometry. Data are expressed as mean ± SEM ($n = 6$ for each group). (G) CD8⁺ T cell percentage in CD45⁺ after anti-CD8 antibody treatment in subcutaneous tumor in MARCO knockdown group. Data are expressed as mean ± SEM ($n = 6$ in each group). (H) Hepa1-6 cells mixed with macrophages (MARCO knockdown) (2:1 ratio) were subcutaneously inoculated into C57BL/6 mice to establish tumor models, treated with anti-CD8 antibody (12.5 mg/kg, intraperitoneal injection every 3 d from the third day), and tumor growth was monitored regularly. Tumor volume data were expressed as mean ± SEM ($n = 6$ in each group) and isotype was IgG2. * $p < 0.05$; ** $p < 0.01$; *** $p < 0.001$; **** $p < 0.0001$.

2.5. Elisa assay

Mouse IFN-beta (Raybiotech, ELM-IFNB1-1), MIG (Raybiotech, ELM-MIG-1), CRG-2 (Raybiotech, LM-CRG2-1), IL-12 (Raybiotech, ELM-IL12P40P70-1), 2'3'-cGAMP (Cayman, 501700) ELISA KIT, and Enhanced ATP Assay Kit (Beyotime, S0027) were used to determine IFN- β , CXCL9, CXCL10, IL12, 2'3'-cGAMP, and ATP concentration in accordance with the instructions provided by the manufacturer.

2.6. IHC, immunofluorescence, and immunoblotting assay

IHC or immunofluorescence staining was performed on 3-mm slides, and the images were evaluated by two independent pathologists. The immunoblotting and IHC procedures are detailed in the Supplementary Materials.

2.7. Quantitative RT-PCR

SYBR qPCR Master Mix (Vazyme, Q711-02) was used to perform real-time quantitative PCR after total RNA extraction and complementary DNA reverse transcription according to the manufacturer's instructions. We compared gene expression levels between the groups using the threshold cycle value. Independent experiments were repeated at least thrice. Table S2 lists the primers used.

2.8. Statistical approach

An analysis of flow cytometry data was carried out using FlowJo.10 (TreeStar, Ashland, OR). GraphPad Prism 9 (La Jolla, CA) was used for statistical analyses. Statistical comparisons between groups were performed using Student's two-tailed t-tests. An analysis of Kaplan–Meier survival curves was performed using log-rank tests. $P < 0.05$ was considered statistically significant. (* $P < 0.05$; ** $P < 0.01$; *** $P < 0.001$; **** $P < 0.0001$).

3. Results

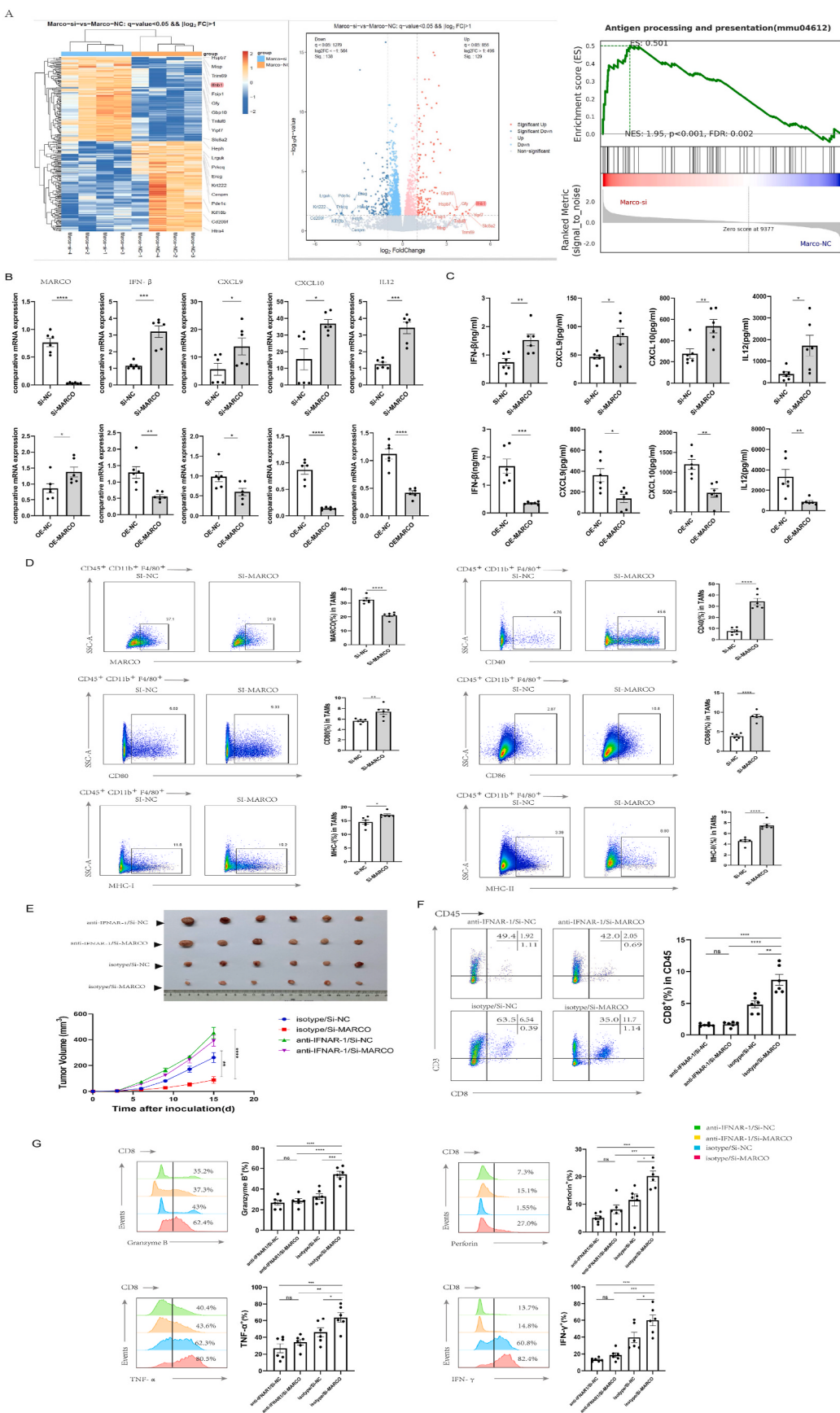
3.1. MARCO was primarily expressed on the HCC microenvironment macrophage surface and was negatively correlated with patient prognosis

We found that MARCO was mainly expressed on the surface of macrophages in the tumor microenvironment of liver cancer by analyzing four datasets from the TISCH database (Fig. 1A) and the data of scRNA seq (Fig. S1). However, the effect of MARCO-expressing macrophages on the progression and prognosis of HCC has received little attention. Therefore, we conducted an in-depth investigation of this group of macrophages. First, we performed immunohistochemical staining on the pathological samples from 121 patients with HCC and

integrated the results with their clinical data. The expression of MARCO in tumor tissue was found to be positively correlated with tumor progression (Fig. 1B). Furthermore, we found that MARCO was concentrated on the surface of macrophages in immunofluorescence staining of samples from these patients, and patients with HCC had more MARCO⁺ TAM infiltration in the TNM (III, IV) phase than that in the TNM (III, IV) phase (Fig. 1C). The infiltration of CD8⁺ T cells into the tumor microenvironment is often closely related to the prognosis of patients with the specific killing of tumor cells [24,25]. We found that the more MARCO⁺ TAMs infiltrate the tumor, the less the number of CD8⁺ T cells, while the killing function of CD8⁺ T cells decreases, and apoptosis increases (Fig. 1D and E). This indicates that MARCO⁺ TAMs are closely related to CD8⁺ T infiltration and function. Survival analysis revealed that patients with HCC with high levels of MARCO⁺ TAM infiltration had lower overall survival and tumor-free survival (Fig. 1F). Therefore, MARCO⁺ TAMs may contribute to tumor progression and poor prognosis by lowering CD8⁺ T cell infiltration and inhibiting their function.

3.2. MARCO⁺ TAMs mediated HCC progression by inhibiting CD8⁺ T cell infiltration and inducing its dysfunction

To better understand the effect of MARCO⁺ TAMs in the progression of HCC, we created a mouse model of subcutaneous tumor formation by co-injecting hepa1-6 cells with mouse bone marrow-derived macrophages (BMDMs) that knocked down MARCO (Si-MARCO) or overexpressed MARCO (OE-MARCO). MARCO on the surface of intratumoral TAM was successfully knocked down or overexpressed based on immunohistochemical findings (Fig. 2A), immunofluorescence assay (Fig. S2A) and flow cytometry analysis (Fig. S2B). Furthermore, by regularly observing the tumor volume of the control (Si-NC + hepa1-6 or OE-NC + hepa1-6) and experimental groups (Si-MARCO + hepa1-6 or OE-MARCO + hepa1-6), compared to the control group, we found that the tumor growth was delayed and the volume decreased significantly in the MARCO knockdown group, while the tumor growth was accelerated and the volume increased significantly in the MARCO overexpression group, indicating that MARCO⁺ TAMs has an obvious tumor-promoting effect (Fig. 2B). We then explored the relationship between MARCO⁺ TAM and CD8⁺ T cells in mouse tumors. We found that after the knockdown of MARCO expressed by macrophages increased, the number of CD8⁺ T cells infiltrating the tumor microenvironment increased significantly, which is consistent with our findings in patients with liver cancer (Fig. 2C). Furthermore, flow cytometry also confirmed that the number of infiltrating CD8⁺ T cells in the tumor tissues was negatively correlated with MARCO⁺ TAMs (Fig. 2D). In addition, when MARCO was overexpressed on the surface of TAMs, CD8⁺ T cell exhaustion increased and the ratio of stem-like CD8⁺ T cells decreased, whereas the exhaustion ratio decreased and the stem-like subpopulation increased when MARCO was knocked down. (Fig. 2E, Fig. S2D). Simultaneously, the



(caption on next page)

Fig. 3. MARCO⁺ TAMs mediate the pro-tumor effects by inhibiting IFN- β secretion.

(A) Transcriptome sequencing was performed on MARCO-NC and MARCO-Si. The left side shows the differential gene heat map of sequencing results, the middle shows the volcano map, and the right shows the GSEA results.

(B) Hepa1-6 cells (pretreated with X-ray irradiator, 30GY, 20 min) and macrophages (MARCO knockdown or overexpression) were co-incubated in a 1:1 ratio for 24 h. Macrophages were selected using flow cytometry to detect the corresponding changes of IFN- β , CXCL9, CXCL10, and IL12 using qPCR. Data are expressed as mean \pm SEM ($n = 6$ for each group).

(C) Hepa1-6 cells (pretreated with X-ray irradiator, 30GY, 20 min) were co-incubated with macrophages (MARCO knockdown or overexpression) in a ratio of 1:1 for 48 h. IFN- β , CXCL9, CXCL10, and IL12 levels in the supernatant were detected using ELISA. Data are expressed as mean \pm SEM ($n = 6$ per group).

(D) Hepa1-6 cells (pretreated with X-ray irradiator, 30GY, 20 min) were co-incubated with macrophages (MARCO knockdown or overexpressed) in a ratio of 1:1 for 48 h. Flow cytometry was performed to analyze the percentage of antigen-presenting molecules (MHC-I⁺, MHC-II⁺, CD40⁺, CD80⁺ and CD86⁺) in macrophages (CD45⁺CD11b⁺F4/80⁺ labeling). Data are expressed as mean \pm SEM ($n = 6$ per group).

(E) Hepa1-6 cells mixed with macrophages (MARCO knockdown) (2:1 ratio) were subcutaneously inoculated into C57BL/6 mice to establish tumor models, treated with anti-IFNB1 receptor blockers (25 mg/kg, multipoint intra-tumor injection every 3 d starting from the third day), and tumor growth was regularly monitored. Tumor volume data are expressed as mean \pm SEM ($n = 6$ in each group), and the isotype was IgG1.

(F) Percentage of CD8⁺T cells in CD45⁺ after anti-IFNB1 blocker treatment in the MARCO knockdown group. Data are expressed as mean \pm SEM ($n = 6$ in each group).

(G) CD8⁺T cells were isolated and enriched after anti-IFNB1 blocker treatment in subcutaneous tumors in MARCO knockdown group. Flow cytometry was used to analyze the cytotoxic function (granzyme B⁺, perforin⁺, TNF- α ⁺, and IFN- γ ⁺ labeling) of CD8⁺T cells. Data are expressed as mean \pm SEM ($n = 6$ for each group). * $p < 0.05$; ** $p < 0.01$; *** $p < 0.001$; **** $p < 0.0001$.

tumor-killing function of CD8⁺T cells, including the secretion of perforin, granzyme, IFN- γ , and TNF- α , was negatively correlated with MARCO⁺TAMs (Fig. 2F). To evaluate the direct effect of MARCO⁺TAM on CD8⁺T cells, we analyzed the cross-priming activity of BMDMs with MARCO knockdown or overexpression by ELISPOT assays measuring of IFN- γ -Secreting CD8⁺T Cells. The results demonstrated that the number of IFN- γ ⁺ spots increased markedly in MARCO knockdown group. On the contrary, it decreased significantly in MARCO overexpression group, indicating a stronger antigen presentation ability of BMDMs with MARCO knockdown (Fig. S2C). In addition, to evaluate the function of NK cells which also play a significantly role in tumor elimination, we detect the expression level of NKG2A, NKG2D, Granzyme B and Perforin in NK cells in mouse subcutaneous tumor model and orthotropic models treated with MARCO mAb (Anti-MARCO), and found little difference of the expression level of these markers among these groups (Figs. S2E–F). To further investigate the role of CD8⁺T cells in MARCO⁺TAM-mediated tumor progression, we used a CD8 monoclonal antibody to knockout CD8⁺T cells in mice (Fig. 2G). We found that the knockout of CD8⁺T cells reversed the inhibitory effect of MARCO knockdown on the surface of TAMs on tumor growth by observing the volume of the tumor and drawing a growth curve. This suggests that MARCO⁺TAM mediates the growth and progression of liver cancer by inhibiting the infiltration and function of CD8⁺T cells (Fig. 2H).

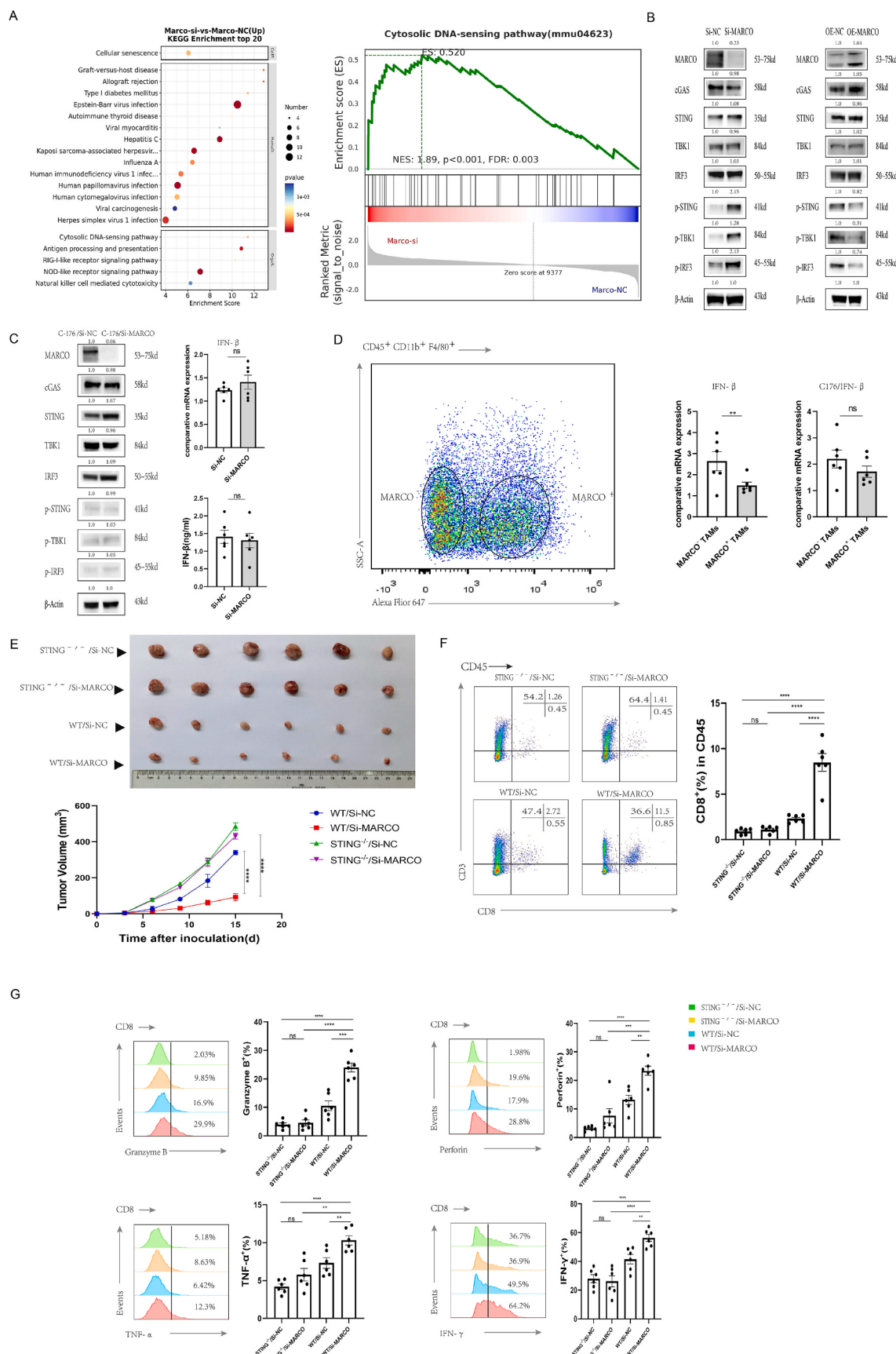
3.3. MARCO⁺ TAMs mediated pro-tumor effects by inhibiting IFN- β secretion

We then explored how MARCO⁺TAMs affect the infiltration and function of CD8⁺T cells. In the experimental group, we initially used small interfering RNA to knock down the MARCO molecule (MARCO-Si) on the surface of BMDM before co-incubating with hepa1-6 cells at a 1:1 ratio for 24 h. The knockdown control BMDM was then co-incubated with hepa1-6 cells as the control group (MARCO-NC). Transcriptome sequencing of the two groups of cells revealed a significant number of differentially expressed genes. We found that the IFN- β score ranked high in the heat map and volcano map analyses, and GSEA revealed that the antigen presentation pathway of macrophages changed significantly (Fig. 3A). IFN- β , as a type I interferon, can boost the secretion of corresponding cytokines, enhance the antigen-presenting function of macrophages and activate the innate and adaptive immune response of the body [26,27]. Therefore, we speculated that MARCO⁺TAMs would promote tumor growth by inhibiting type I interferon secretion and blocking antigen-presenting pathway activation. Hence, we flow sort the macrophages from the co-culture system, detected the expression levels of IFN- β , CXCL9, CXCL10, and IL12 using qPCR, and collected the supernatant to verify the protein level using ELISA. Consistent with the results of transcriptional group, the expression level of IFN- β and a

series of downstream cytokines in macrophages with low MARCO in co-culture system were significantly increased, while macrophages overexpressing MARCO were on the contrary (Fig. 3B and C). Flow cytometry was used to detect the expression of macrophage surface costimulatory molecules CD40, CD80, and CD86 as well as antigen-presenting molecules MHC-I and MHC-II. These findings were consistent with our hypothesis that MARCO knockdown significantly increased the expression of antigen presentation and co-stimulatory molecules, whereas MARCO overexpression decreased (Fig. 3D). To verify the important role of IFN- β in MARCO⁺TAMs-mediated immunosuppression, we blocked the receptor IFNAR1 of IFN- β with a specific neutralizing antibody. The analysis of tumor volume and growth curves revealed that, compared to the control group, anti-IFNAR1 therapy significantly attenuated tumor growth inhibition (Fig. 3E) due to MARCO knockdown. Simultaneously, using flow cytometry, we found that blocking the type I interferon receptor IFNAR1 partly inhibited the increase in CD8⁺T cell infiltration and function enhancement caused by knocking down the expression of TAMs MARCO (Fig. 3F and G). Therefore, the tumor-promoting effect of MARCO⁺TAMs was dependent on IFN- β .

3.4. MARCO⁺ TAMs mediated IFN- β secretion decrease by inhibiting STING activation

The preceding experiments revealed that MARCO suppressed IFN- β secretion from TAMs; therefore, we explored how IFN- β expression is inhibited. MARCO knockdown significantly activated the intracellular DNA-sensing pathway of macrophages based on further analysis of the above transcriptome results (Fig. 4A). The cyclic GMP-AMP synthase (cGAS)-STING pathway is a classic intracellular DNA sensing pathway that activates type I interferon secretion [28,29]. Therefore, we used a western blot assay to assess cGAS-STING pathway activation in TAMs with knockdown and overexpression. After MARCO knockdown or overexpression, the total amount of intracellular cGAS, STING, TBK1, and IRF3 proteins did not change significantly. However, after MARCO knockdown, phosphorylation of intracellular STING protein was significantly enhanced, as was the phosphorylation of downstream TBK1 and IRF3 proteins, while overexpression of MARCO was reduced (Fig. 4B). Therefore, we speculated that MARCO⁺TAMs could inhibit the activation of the intracellular STING pathway and mediate the decrease in IFN- β secretion. To test this hypothesis, we administered the STING blocker C-176 to a co-culture system of hepa1-6 cells and BMDM for 48 h. We found that compared to the control group, STING blockers significantly inhibited STING pathway activation and IFN- β expression in MARCO knockdown macrophages (Fig. 4C). We further verified the role of the STING pathway in MARCO⁺TAMs in mice. We injected hepa1-6 cells into mice with *in situ* tumor formation, flow-sorted the



(caption on next page)

Fig. 4. MARCO-mediated IFN- β secretion decrease by inhibiting STING activation.

- (A) The KEGG pathway enrichment analysis of the differential genes in the transcriptome revealed differences in cytosolic DNA sensing pathways.
- (B) Western blotting analysis of Sting pathway-related proteins in macrophages (MARCO knockdown or overexpressed) after incubating with Hepa1-6 cells (pretreated with X-ray irradiator, 30GY, 20 min) in a 1:1 ratio for 48 h
- (C) Hepa1-6 cells (pretreated with X-ray irradiator, 30GY, 20 min) were co-incubated with macrophages (MARCO knockdown) in a 1:1 ratio. Following 48 h of treatment with Sting blocker C-176 (100 μ g/ml), a western blot analysis of proteins associated with the Sting pathway was performed (left figure). IFN- β changes were detected using qPCR and ELISA (right figure).
- (D) C57BL/6 mice were inoculated with Hepa1-6 cells *in situ* to establish a tumor model, and C-176 was treated (10 mg/kg, daily intraperitoneal injection). MARCO $^+$ TAMs and MARCO $^-$ TAMs were separated from tumor tissues *in situ* with or without C-176 using flow cytometry 14 d later. IFN- β changes were detected using qPCR. Data are expressed as mean \pm SEM ($n = 6$ in each group).
- (E) Hepa1-6 cells mixed with macrophages (MARCO knockdown) (2:1 ratio) were inoculated subcutaneously with Sting $^-/-$ and WT mice to establish tumor models, and tumor growth was regularly monitored. Tumor volume data are expressed as mean \pm SEM ($n = 6$ for each group).
- (F) Flow cytometry was used to analyze CD8 $^+$ T cells percentage in CD45 $^+$ in subcutaneous tumors in the MARCO knockdown group of Sting $^-/-$ and WT mice. Data are expressed as mean \pm SEM ($n = 6$ in each group).
- (G) CD8 $^+$ T cells were isolated and enriched from subcutaneous tumors of Sting $^-/-$ and WT mice in MARCO knockdown group. Flow cytometry was used to analyze CD8 $^+$ T cell cytotoxic function (granzyme B $^+$, perforin $^+$, TNF- α $^+$, IFN- γ $^+$ labeling). Data are expressed as mean \pm SEM ($n = 6$ for each group). * $p < 0.05$; ** $p < 0.01$; *** $p < 0.001$; **** $p < 0.0001$.

◀

MARCO $^+$ and MARCO $^-$ macrophages from the tumor microenvironment, and compared their IFN- β expression levels. Consistent with our *in vitro* results, the qPCR results revealed that IFN- β expression of MARCO-TAMs in hepatoma tumors of mice not injected with C-176 was significantly higher than that in MARCO $^+$ TAMs. In contrast, the difference in IFN- β expression induced by MARCO (Fig. 4D) was eliminated in mice injected with C-176. Finally, we verified the role of the STING pathway in MARCO-mediated tumor progression in STING knockout mice (Sting $^-/-$). Compared to wild-type mice, STING knockout significantly eliminated the inhibitory effect of MARCO knockout on tumor growth. It reversed the increased CD8 $^+$ T cell infiltration and the functional enhancement caused by MARCO knockdown (Fig. 4E–G). Therefore, the STING pathway is crucial in the MARCO-mediated inhibition of IFN- β secretion.

3.5. MARCO inhibited cGAMP transport from tumor cells into TAMs via P2X7R

Apoptosis of cancer cells increases in malignant solid tumors, especially HCC, due to the excessive proliferation of tumor cells and the formation of a hypoxic environment [30]. Most apoptotic cells will be ingested by phagocytes, such as macrophages, before their capsules are broken. This process is called immune quiescence [31]. Phagocytes also ingest apoptotic tumor cells, eliminating various substances that can activate the immune system. Therefore, blocking phagocytic receptors on the surface of macrophages can lead to the release of immune-activating substances, such as ATP and cGAMP, in tumors, thus enhancing the anti-tumor immune response of the body [32]. Therefore, we speculated that MARCO, a scavenger receptor on the surface of macrophages, would similarly inhibit antitumor immunity activation by promoting apoptotic tumor cell clearance. Therefore, we labeled Hepa1-6 cells with CFSE, induced apoptosis of hep1-6 cells via cell irradiation, and co-incubated them with MARCO-knockdown macrophages and the control group. Flow cytometry was used to detect the proportion of remaining apoptotic tumor cells and macrophage phagocytosis of CFSE-labeled tumor cells in the co-culture system. We found that MARCO could stimulate the macrophage phagocytosis of apoptotic tumor cells (Fig. 5A and B).

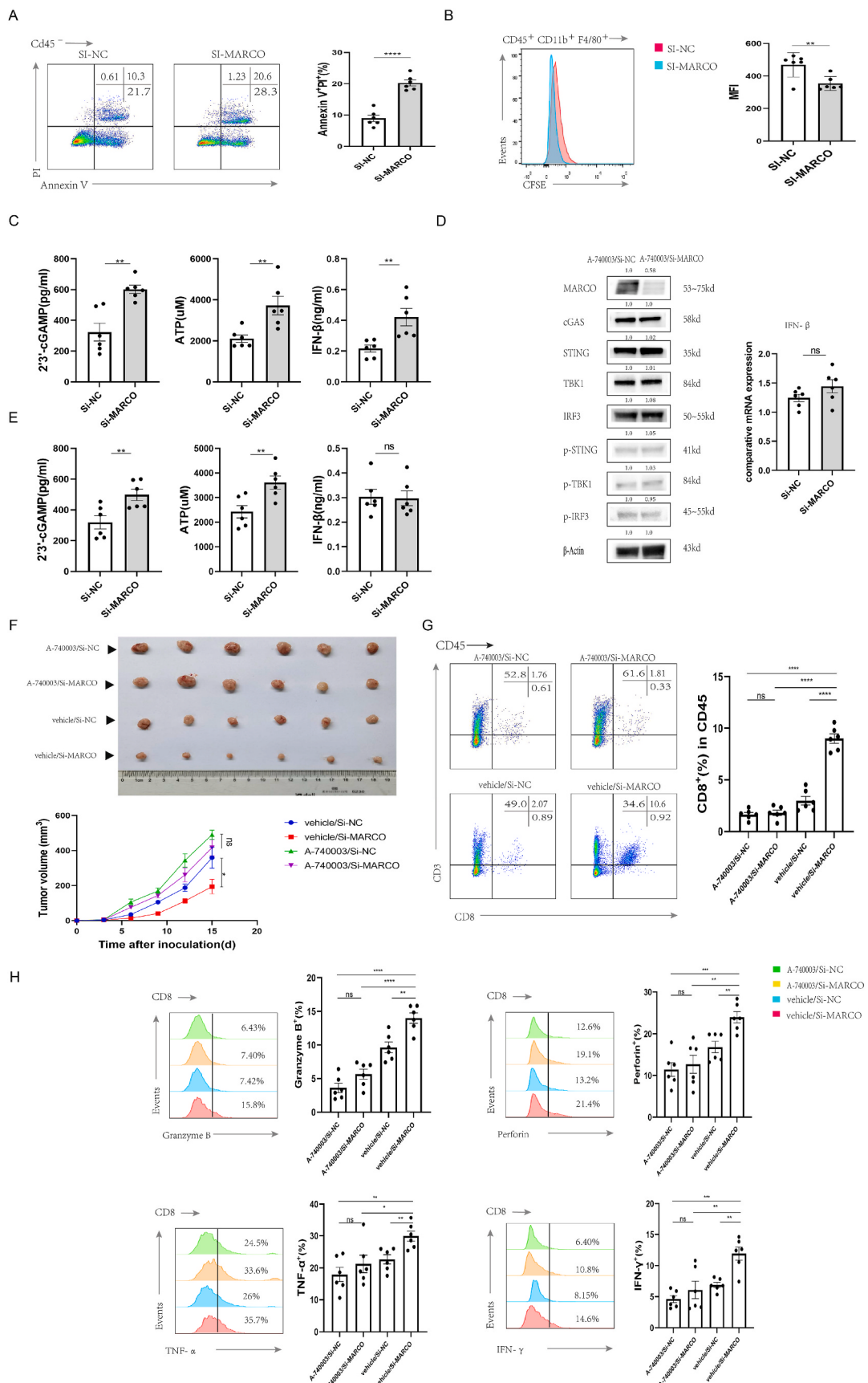
Several studies have revealed that because of the rupture of their own nuclear or mitochondrial membranes, the release of DNA from apoptotic tumor cells activates their intracellular cGAS and produces a large amount of cGAMP, which can then enter macrophages via the ATP-dependent receptor P2X7R on the cell membrane and activate the downstream STING pathway [32–35]. Therefore, we examined the supernatant of apoptotic hep1-6 cells co-incubated with macrophages. Compared to the control group, MARCO knockdown significantly increased the contents of cGAMP and ATP in the supernatant, it also significantly increased IFN- β secretion level (Fig. 5C). To test the effect

of phagocytic ability of TAMs on the content of cGAMP and ATP in supernatants of co-culturing system released by dying tumor cells, BMDMs with MARCO knocking down or control BMDMs were separated from irradiated-tumor cells via a *trans-well* screen that only allows particles under 0.4 μ m in diameter to travel freely between compartments. Under these setting, there was no significant difference in the content of cGAMP and ATP in supernatants between the MARCO knocking down or control BMDMs groups (Fig. S3A), indicating MARCO $^+$ TAM mediated-increased level of cGAMP and ATP is dependent on direct cell-cell contact. Furthermore, the addition of Latrunculin B, an actin polymerization inhibitor, to restrain the phagocytic ability of BMDMs in the co-culture system also led to no significant difference in the content of cGAMP and ATP in supernatants between the MARCO knocking down or control BMDMs groups (Fig. S3B). Production of IFN- β by BMDMs in response to irradiated tumor cells also did not demonstrate significant difference between the two groups (Figs. S3A–B). Taken together, these results suggest that the increased level of cGAMP and ATP were dependent on the decreased phagocytic ability of MARCO knocking down TAMs. To verify the role of P2X7R, we added the P2X7R antagonist A-740003 to the co-culture system and isolated macrophages. Using qPCR and western blotting, we found that A740003 reversed the activation effect of MARCO knockdown on the STING pathway (Fig. 5D). Simultaneously, while there were still changes in the levels of ATP and cGAMP in the supernatant of the co-culture system, there was no statistical difference in IFN- β secretion (Fig. 5E), indicating that P2X7R played a significant role in IFN- β secretion inhibition mediated by MARCO.

Finally, the mice experiment confirmed the role of P2X7R in tumor immunosuppression by MARCO $^+$ macrophages in mice. We found that blocking P2X7R significantly reversed the effect of MARCO knockdown on tumor growth inhibition, CD8 $^+$ T cell infiltration, and functional enhancement (Fig. 5F–H). Therefore, we confirmed that MARCO $^+$ macrophages downregulated antitumor immunity by inhibiting P2X7R transport to tumor-derived cGAMP.

3.6. Blocking MARCO with antibodies significantly improved the anti-tumor immune response and enhanced liver cancer response to PD-L1 therapy

CD8 $^+$ T cell infiltration and function in tumors are critical for the efficacy of anti-PD-L1 and other immune checkpoint-blocking therapies [36,37]. Previously, we found that knocking down MARCO on the surface of TAMs significantly increased CD8 $^+$ T cell infiltration number and function in HCC. Therefore, we created a MARCO-blocking antibody (HUABIO_20230221) and validated the effectiveness of it (Fig. S4). Consistent with our previous results, we demonstrated that the P2X7R-STING-IFN- β axis could be inhibited in orthotopic tumor model with the application of MARCO-blocking antibody (Figs. S5–7). Then we



(caption on next page)

Fig. 5. MARCO inhibits cGAMP transport from tumor cells into TAMs via the P2X7R pathway, activating its STING–IFN- β pathway.
 (A) Hepa1-6 cells were treated with an X-ray irradiator (30GY, 20 min) and mixed with macrophages (MARCO knockdown) for co-incubation (1:1) for 48 h. Hepa1-6 cell apoptosis (CD45 $^-$ PI $^+$ AN $^+$ labeled) was analyzed using flow cytometry. Data are expressed as mean \pm SEM (n = 6 for each group).
 (B) CFSE-labeled Hepa1-6 cells were treated with an X-ray irradiator (30GY, 20 min) and mixed with macrophages (MARCO knocked down) for co-incubation (1:1 ratio) for 48 h. Macrophage phagocytic necrotic tumor cells (CD45 $^+$ CD11b $^+$ F4/80 $^+$ labeling) were analyzed using flow cytometry (marked by CFSE mean immunofluorescence intensity MFI). Data are expressed as mean \pm SEM (n = 6 per group).
 (C) Hepa1-6 cells were treated with an X-ray irradiator (30GY, 20 min) and mixed with macrophages (MARCO knocked down) for co-incubation (1:1) for 48 h. Supernatant ELISA was performed to detect 2'3'-cGAMP, ATP, and IFN- β levels. Data are expressed as mean \pm SEM (n = 6 for each group).
 (D) Hepa1-6 cells were treated with an X-ray irradiator (30GY, 20 min) and mixed with macrophages (MARCO knocked down) for co-incubation (ratio 1:1). P2X7R receptor blocker A-740003 (100 μ M) was added for 48 h. Macrophages were sorted using flow cytometry. Sting pathway-related proteins were analyzed using western blotting, and the changes of IFN- β were detected using qPCR. Data are expressed as mean \pm SEM (n = 6 in each group).
 (E) Hepa1-6 cells were treated with an X-ray irradiator (30GY, 20 min) and mixed with macrophages (MARCO knockdown) for co-incubation (1:1 ratio). A-740003 (100 μ M) was added for 48 h. ELISA was used to detect 2'3'-cGAMP, ATP, and IFN- β levels in the supernatant. Data are expressed as mean \pm SEM (n = 6 in each group).
 (F) C57BL/6 mice were subcutaneously inoculated with Hepa1-6 cells mixed with macrophages (MARCO knockdown) (ratio of 2:1) to establish tumor models. A-740003 was administered (50 mg/kg, intraperitoneal injection every 3 d starting from the third day), and tumor growth was regularly monitored. Tumor volume data are expressed as mean \pm SEM (n = 6 in each group).
 (G) CD8 $^+$ T cell percentage in CD45 $^+$ cells in subcutaneous tumors were analyzed following treatment with A-740003 in MARCO knockdown group. Data are expressed as mean \pm SEM (n = 6 in each group).
 (H) CD8 $^+$ T cells were isolated and enriched from subcutaneous tumors after A-740003 treatment in MARCO knockdown group. Flow cytometry was used to analyze the cytotoxic function of CD8 $^+$ T cells (granzyme B $^+$, perforin $^+$, TNF- α $^+$, and IFN- γ $^+$ labeling). Data are expressed as mean \pm SEM (n = 6 for each group). *p < 0.05; **p < 0.01; ***p < 0.001; ****p < 0.0001.

used it in combination with a PD-L1 antibody to verify whether the efficacy of anti-PD-L1 therapy could be enhanced by specifically blocking MARCO $^+$ macrophage subsets. According to the *in situ* tumor formation model results in mice, anti-MARCO and anti-PD-L1 therapies had obvious synergistic effects and significantly inhibited HCC growth (Fig. 6A). We found that the MARCO-blocking antibody increased the infiltration and function of CD8 $^+$ T cells in the tumor using flow cytometry. The combined use of MARCO and PD-L1 antibodies significantly increased the number of CD8 $^+$ T cell infiltration, and its tumor-killing effect was stronger than that of MARCO or PD-L1 antibodies alone (Fig. 6B and C). Furthermore, survival analysis of tumor-bearing mice revealed that combination therapy significantly improved mice prognosis (Fig. 6D). Therefore, targeting MARCO $^+$ macrophages can significantly improve the efficacy of anti-PD-L1 therapy for liver cancer and it is expected to become a novel potential target for combined immune checkpoint inhibitor therapy.

4. Discussion

The main mechanism for killing tumor cells is infiltrating CD8 $^+$ T cells in the tumor microenvironment. However, tumor cells develop an immunosuppressive tumor microenvironment via a series of mechanisms that evade destruction by CD8 $^+$ T cell death. Conventional immune checkpoint inhibitors often target pathways associated with CD8 $^+$ T cell activation and function while ignoring many innate immune cells in the tumor microenvironment. Numerous studies have revealed that most TAMs in the tumor microenvironment have high immunosuppressive abilities; however, due to their heterogeneity, they require more accurate investigation in future studies. We found that a group of macrophages with high MARCO expression levels could promote the occurrence and progression of HCC by reducing CD8 $^+$ T cell infiltration and inhibiting their tumor-killing ability in the microenvironment of HCC. Previous studies have revealed that MARCO $^+$ macrophages can modify the immune microenvironment of tumors by inhibiting NK cell function in melanoma, promoting the infiltration of Treg cells in non-small cell lung cancer, and inhibiting killer T and NK cell infiltration [20,38]. However, there are few studies on how MARCO $^+$ TAMs alter the infiltration and function of these cells, and the specific mechanism remains unclear.

To the best of our knowledge, this is the first study to report that the tumor-promoting effect of MARCO $^+$ TAMs is related to type I interferon IFN- β . That is, macrophages with high MARCO expression levels tend to express low IFN- β levels, inhibiting TAM antigen presentation and

specific immune activation. Type I interferon was first discovered for its antiviral properties, and its immunomodulatory effect and role in non-viral pathogen infections are gaining increasing attention [39]. Type I interferons can directly inhibit tumor growth, promote apoptosis, and kill tumor cells indirectly by activating immune cells [40,41]. However, because IFN- β expression is low in the tumor environment, its mechanism of action is likely to promote macrophage tumor antigen presentation via an autocrine signaling pathway. Further, as the downstream of IFN- β , MHC-I and MHC-II expression on the surface of TAMs with high MARCO expression decreased significantly, as did the costimulatory molecules CD80, CD86, and CD40, whereas IL-12, CXCL9, and CXCL10 secretions from macrophages decreased, resulting in reduced recruitment, infiltration and limited CD8 $^+$ T cell activation, which is consistent with our findings.

However, given that the intracellular structure of MARCO is compact and contains almost no intracellular signal domain, it will be an attractive research direction to explore how MARCO $^+$ macrophages inhibit IFN- β secretion. The structure of MARCO indicates that regulating its expression via intracellular signal transduction, such as pattern recognition receptors, is challenging. Our findings revealed that MARCO $^+$ macrophages limit IFN- β secretion via the intracellular DNA sensing pathway. cGAS is a classic intracellular DNA-sensing protein that catalyzes the reaction of ATP and GTP to produce cGAMP in response to double-stranded DNA stimulation. cGAMP then functions as a second messenger, activating the downstream STING to enhance type I interferon secretion [28,42,43]. STING activation in immune cells can be induced by cGAMP catalyzed by self-cGAS or exogenous cGAMP entering the cell via transporters on the cell membrane. In the tumor microenvironment, some studies have revealed that tumor-derived cGAMP can be released into the extracellular space, which is an important method for immune cells to activate STING [33,44]. However, TAMs quickly digest dying tumor cells, decreasing ATP and cGAMP generated by tumor cells in the tumor microenvironment [32]. Among them, TAMs with high MARCO expression revealed enhanced phagocytosis and inhibited tumor-derived cGAMP activation of intracellular STING. According to a study, tumor-derived cGAMP can also be transported into NK cells in the tumor microenvironment to enhance their tumor-killing ability. This may explain why using MARCO antibodies in some tumors can improve NK cell function [20,38,45]. The inhibitory effect of MARCO $^+$ TAM on IFN- β expression was found to be significantly dependent on the cGAMP transport channel P2X7R on the surface of TAM. P2X7R is an ATP-activated transport channel; however, due to the clearance of dead tumor cells by MARCO $^+$ TAM, the decrease in ATP in

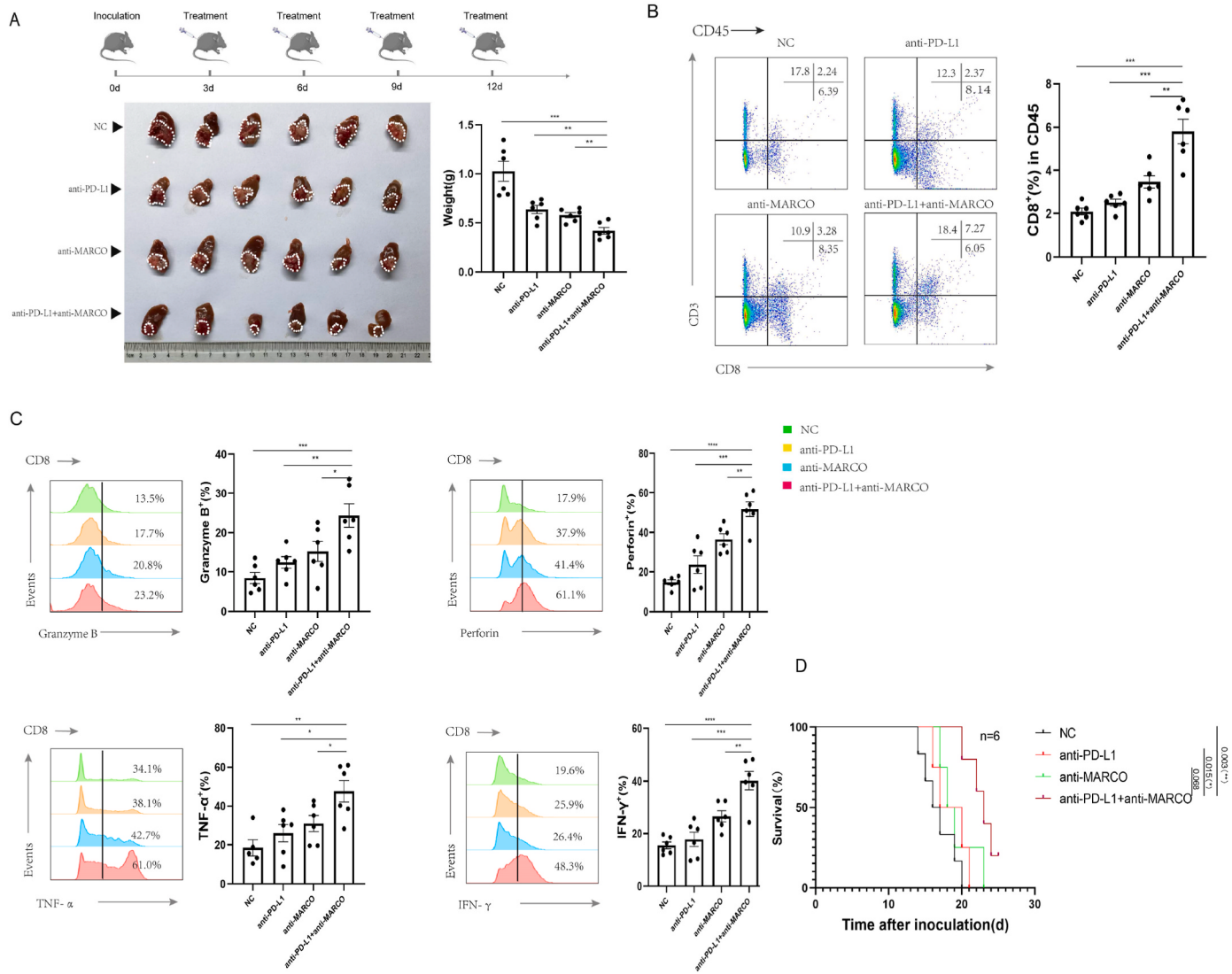


Fig. 6. Blocking MARCO with antibodies significantly improves the anti-tumor immune response and enhances liver cancer response to PD-L1 therapy
 (A) In situ inoculation of Hepa1-6 cells was performed on C57BL/6 mice in order to establish tumor models, which were randomly divided into four groups: NC, anti-MARCO antibody treatment (5 mg/kg, intraperitoneal injection every 3 d from the 3rd day), anti-PD-L1 antibody treatment (20 mg/kg, intraperitoneal injection every 3 d from the 3rd day), and anti-PD-L1 antibody + anti-MARCO antibody combined treatment groups. Tumor weight data are expressed as mean \pm SEM (n = 6 per group).

(B) CD8⁺ T cell percentage in CD45⁺ cells from four groups of orthotopic tumors was analyzed using flow cytometry. Data are expressed as mean \pm SEM (n = 6 in each group).

(C) CD8⁺ T cells were isolated and enriched from four groups of orthotopic tumors. The cytotoxic function (granzyme B⁺, perforin⁺, TNF-α⁺, IFN-γ⁺ labeling) of CD8⁺ T cells was analyzed using flow cytometry. Data are expressed as mean \pm SEM (n = 6 per group).

(D) Total survival analysis of four groups of mice (n = 6 per group). *p < 0.05; **p < 0.01; ***p < 0.001; ****p < 0.0001.

the tumor microenvironment inhibits P2X7R activation, making tumor-derived cGAMP difficult to enter the TAM-activated type I interferon response and ultimately promoting the formation of inhibitory tumor immune microenvironment.

Previous studies have revealed that CD8⁺ T cell infiltration and function in the tumor microenvironment are often required for determining immune checkpoint-blocking therapy [37]. We found that MARCO⁺ macrophages in HCC inhibited CD8⁺ T cell infiltration and function by inhibiting the type I interferon response, which might be the reason behind HCC not responding well to anti-PD-L1 therapy alone. Therefore, we blocked its function as an anti-MARCO antibody and found that CD8⁺ T cell infiltration in the tumor microenvironment was significantly increased, as was CD8⁺ T cell function, including granzyme, perforin, IFN-γ, and TNF-α secretion. The combination of anti-MARCO

and anti-PD-L1 antibodies exhibited a significant synergistic effect and significantly slowed liver cancer progression. Thus, our study provides a novel combination regimen for immune checkpoint therapy to improve the sensitivity and response rate of patients with liver cancer.

Our studies have some limitations. In our studies, STING^{-/-} suppressed MARCO⁺ macrophage-mediated immune response both in *in vitro* and *in vivo* assays. However, in *in vivo* assay, STING expression was lacked among all immune subsets in STING^{-/-} mice, which meant that other antigen presenting cell subsets, like DCs, might also be activated by the increased IFN-β, thus contributing to the activation and infiltration of CD8⁺ T cells to some extent. Thus, the roles of main subsets of immune cells in tumor microenvironment in MARCO⁺ macrophage-mediated immunosuppression still calls for further researches to elucidate in the future.

In summary, our study confirmed, for the first time, that the immunosuppressive effect of MARCO⁺TAMs is formed by inhibiting IFN- β secretion. It also explained its specific mechanism and confirmed the critical role of P2X7R in it. Moreover, blocking the MARCO⁺TAM subpopulation using antibodies can effectively improve the inhibitory tumor immune microenvironment and the efficacy of immune checkpoint therapy, providing a novel potential target for liver cancer immunotherapy.

CRediT authorship contribution statement

Limin Ding: Writing – review & editing, Writing – original draft, Validation, Software, Methodology, Investigation, Formal analysis, Data curation, Conceptualization. **Junjie Qian:** Validation, Methodology, Investigation. **Xizhi Yu:** Validation, Methodology, Investigation. **Qinchuan Wu:** Methodology. **Jing Mao:** Software. **Xi Liu:** Investigation. **Yubo Wang:** Software. **Danjing Guo:** Software, Investigation. **Rong Su:** Software, Investigation. **Haiyang Xie:** Software, Investigation. **Shengyong Yin:** Software, Investigation. **Lin Zhou:** Writing – review & editing, Visualization, Supervision, Resources, Project administration, Funding acquisition, Data curation, Conceptualization. **ShuSen Zheng:** Writing – review & editing, Supervision, Resources, Project administration, Funding acquisition, Conceptualization.

Declaration of competing interest

The authors declare that they have no known competing financial interests or personal relationships that could have appeared to influence the work reported in this paper.

Acknowledgements

This work was supported by the Research Unit Project of the Chinese Academy of Medical Sciences (2019-I2M-5-030); Research Project of Jinan Microecological Biomedicine Shandong Laboratory (JNL-2022008B); Health Commission of Zhejiang Province (JBZX-202004); and the Scientific Research Fund of Zhejiang Provincial Education Department (Y202250768). We thank OE Biotech Co., Ltd. (Shanghai, China) for providing the RNA-seq data used in this study. We thank HUABIO Biotech Co., Ltd. (Hangzhou, China) for neutralizing the anti-MARCO antibody used in this study.

Appendix A. Supplementary data

Supplementary data to this article can be found online at <https://doi.org/10.1016/j.canlet.2023.216568>.

References

- [1] H. Rumgay, M. Arnold, J. Ferlay, O. Lesi, C.J. Cabasag, J. Vignat, M. Laversanne, K.A. McGlynn, I. Soerjomataram, Global burden of primary liver cancer in 2020 and predictions to 2040, *J. Hepatol.* 77 (2022) 1598–1606.
- [2] S. Qin, S.L. Chan, S. Gu, Y. Bai, Z. Ren, X. Lin, Z. Chen, W. Jia, Y. Jin, Y. Guo, X. Hu, Z. Meng, J. Liang, Y. Cheng, J. Xiong, H. Ren, F. Yang, W. Li, Y. Chen, Y. Zeng, A. Sultanbaev, M. Pazgan-Simon, M. Pisetska, D. Melisi, D. Ponomarenko, Y. Osypchuk, I. Sinielnikov, T.S. Yang, X. Liang, C. Chen, L. Wang, A.L. Cheng, A. Kaseb, A. Vogel, C.-S. Group, Camrelizumab plus rivooceranib versus sorafenib as first-line therapy for unresectable hepatocellular carcinoma (CARES-310): a randomised, open-label, international phase 3 study, *Lancet* 402 (2023) 1133–1146.
- [3] Z. Tan, M.S. Chiu, X. Yang, M. Yue, T.T. Cheung, D. Zhou, Y. Wang, A.W. Chan, C. W. Yan, K.Y. Kwan, Y.C. Wong, X. Li, J. Zhou, K.F. To, J. Zhu, C.M. Lo, A.S. Cheng, S.L. Chan, L. Liu, Y.Q. Song, K. Man, Z. Chen, Isoformic PD-1-mediated immunosuppression underlies resistance to PD-1 blockade in hepatocellular carcinoma patients, *Gut* 72 (2023) 1568–1580.
- [4] A.L. Cheng, C. Hsu, S.L. Chan, S.P. Choo, M. Kudo, Challenges of combination therapy with immune checkpoint inhibitors for hepatocellular carcinoma, *J. Hepatol.* 72 (2020) 307–319.
- [5] Q. Wu, W. Zhou, S. Yin, Y. Zhou, T. Chen, J. Qian, R. Su, L. Hong, H. Lu, F. Zhang, H. Xie, L. Zhou, S. Zheng, Blocking triggering receptor expressed on myeloid cells-1-positive tumor-associated macrophages induced by hypoxia reverses immunosuppression and anti-programmed cell death ligand 1 resistance in liver cancer, *Hepatology* (Baltimore, Md 70 (2019) 198–214.
- [6] J. Qian, T. Chen, Q. Wu, L. Zhou, W. Zhou, L. Wu, S. Wang, J. Lu, W. Wang, D. Li, H. Xie, R. Su, D. Guo, Z. Liu, N. He, S. Yin, S. Zheng, Blocking exposed PD-L1 elicited by nanosecond pulsed electric field reverses dysfunction of CD8(+) T cells in liver cancer, *Cancer Lett.* 495 (2020) 1–11.
- [7] V. Hernandez-Gea, S. Toffanin, S.L. Friedman, J.M. Llovet, Role of the microenvironment in the pathogenesis and treatment of hepatocellular carcinoma, *Gastroenterology* 144 (2013) 512–527.
- [8] F. Ginhoux, M. Guilliams, Tissue-resident macrophage ontogeny and homeostasis, *Immunity* 44 (2016) 439–449.
- [9] M. Kiss, S. Van Gassen, K. Movahedi, Y. Saeyns, D. Laoui, Myeloid cell heterogeneity in cancer: not a single cell alike, *Cell. Immunol.* 330 (2018) 188–201.
- [10] C.E. Lewis, A.S. Harney, J.W. Pollard, The multifaceted role of perivascular macrophages in tumors, *Cancer Cell* 30 (2016) 18–25.
- [11] M. Yang, D. McKay, J.W. Pollard, C.E. Lewis, Diverse functions of macrophages in different tumor microenvironments, *Cancer Res.* 78 (2018) 5492–5503.
- [12] G. Kraal, L.J. van der Laan, O. Elomaa, K. Tryggvason, The macrophage receptor MARCO, *Microb. Infect.* 2 (2000) 313–316.
- [13] F. Granucci, F. Petralia, M. Urbano, S. Citterio, F. Di Tota, L. Santambrogio, P. Ricciardi-Castagnoli, The scavenger receptor MARCO mediates cytoskeleton rearrangements in dendritic cells and microglia, *Blood* 102 (2003) 2940–2947.
- [14] S.A. Thakur, C.A. Beamer, C.T. Migliaccio, A. Holian, Critical role of MARCO in crystalline silica-induced pulmonary inflammation, *Toxicol. Sci. : an official journal of the Society of Toxicology* 108 (2009) 462–471.
- [15] M. Yang, X. Qian, N. Wang, Y. Ding, H. Li, Y. Zhao, S. Yao, Inhibition of MARCO ameliorates silica-induced pulmonary fibrosis by regulating epithelial-mesenchymal transition, *Toxicol. Lett.* 301 (2019) 64–72.
- [16] R. Alarcón, C. Fuenzalida, M. Santibáñez, R. von Bernhardi, Expression of scavenger receptors in glial cells. Comparing the adhesion of astrocytes and microglia from neonatal rats to surface-bound beta-amyloid, *J. Biol. Chem.* 280 (2005) 30406–30415.
- [17] Y. Yamada, T. Doi, T. Hamakubo, T. Kodama, Scavenger receptor family proteins: roles for atherosclerosis, host defence and disorders of the central nervous system, *Cell. Mol. Life Sci. : CMLS* 54 (1998) 628–640.
- [18] Y.S. Yang, X. Jin, Q. Li, Y.Y. Chen, F. Chen, H. Zhang, Y. Su, Y. Xiao, G.H. Di, Y. Z. Jiang, S. Huang, Z.M. Shao, Superenhancer drives a tumor-specific splicing variant of MARCO to promote triple-negative breast cancer progression, *Proc. Natl. Acad. Sci. U.S.A.* 119 (2022), e2207201119.
- [19] M. Masetti, R. Carrasco, F. Portale, G. Marelli, N. Morina, M. Pandini, M. Iovino, B. Partini, M. Erreni, A. Ponsetta, E. Magrini, P. Colombo, G. Elefante, F. S. Colombo, J.M.M. den Haan, C. Peano, J. Cibella, A. Termanini, P. Kunderfranco, J. Brummelman, M.W.H. Chung, M. Lazzeri, R. Hurle, P. Casale, E. Lugli, R. A. DePinho, S. Mukhopadhyay, S. Gordon, D. Di Mitri, Lipid-loaded tumor-associated macrophages sustain tumor growth and invasiveness in prostate cancer, *J. Exp. Med.* 219 (2022).
- [20] L. Lu Fleur, J. Botling, F. He, C. Pelicano, C. Zhou, C. He, G. Palano, A. Mezheyevski, P. Micke, J.V. Ravetch, M.C.I. Karlsson, D. Sarhan, Targeting MARCO and IL37R on immunosuppressive macrophages in lung cancer blocks regulatory T cells and supports cytotoxic lymphocyte function, *Cancer Res.* 81 (2021) 956–967.
- [21] B. Shi, J. Chu, T. Huang, X. Wang, Q. Li, Q. Gao, Q. Xia, S. Luo, The scavenger receptor MARCO expressed by tumor-associated macrophages are highly associated with poor pancreatic cancer prognosis, *Front. Oncol.* 11 (2021), 771488.
- [22] B.R. Bianchi, K.J. Lynch, E. Touma, W. Niforatos, E.C. Burgard, K.M. Alexander, H. S. Park, H. Yu, R. Metzger, E. Kowaluk, M.F. Jarvis, T. van Biesen, Pharmacological characterization of recombinant human and rat P2X receptor subtypes, *Eur. J. Pharmacol.* 376 (1999) 127–138.
- [23] F. Di Virgilio, A.C. Sarti, S. Falzoni, E. De Marchi, E. Adinolfi, Extracellular ATP and P2 purinergic signalling in the tumour microenvironment, *Nat. Rev. Cancer* 18 (2018) 601–618.
- [24] M. St Paul, P.S. Ohashi, The roles of CD8(+) T cell subsets in antitumor immunity, *Trends Cell Biol.* 30 (2020) 695–704.
- [25] A. Gabrielson, Y. Wu, H. Wang, J. Jiang, B. Kallakury, Z. Gatalica, S. Reddy, D. Kleiner, T. Fishbein, L. Johnson, E. Island, R. Satoskar, F. Banovac, R. Jha, J. Kachhela, P. Feng, T. Zhang, A. Tesfaye, P. Prins, C. Loffredo, J. Marshall, L. Weiner, M. Atkins, A.R. He, Intratumoral CD3 and CD8 T-cell densities associated with relapse-free survival in HCC, *Cancer Immunol. Res.* 4 (2016) 419–430.
- [26] L. Zitvogel, L. Galluzzi, O. Kepp, M.J. Smyth, G. Kroemer, Type I interferons in antitumor immunity, *Nat. Rev. Immunol.* 15 (2015) 405–414.
- [27] L.B. Ivashkiv, L.T. Donlin, Regulation of type I interferon responses, *Nature reviews. Immunology* 14 (2014) 36–49.
- [28] L. Deng, H. Liang, M. Xu, X. Yang, B. Burnett, A. Arina, X.D. Li, H. Mauceri, M. Beckett, T. Darga, X. Huang, T.F. Gajewski, Z.J. Chen, Y.X. Fu, R. Weichselbaum, STING-dependent cytosolic DNA sensing promotes radiation-induced type I interferon-dependent antitumor immunity in immunogenic tumors, *Immunity* 41 (2014) 843–852.
- [29] T. Su, Y. Zhang, K. Valerie, X.Y. Wang, S. Lin, G. Zhu, STING activation in cancer immunotherapy, *Theranostics* 9 (2019) 7759–7771.
- [30] P. Vaupel, A. Mayer, Hypoxia in cancer: significance and impact on clinical outcome, *Cancer Metastasis Rev.* 26 (2007) 225–239.
- [31] S. Nagata, Apoptosis and clearance of apoptotic cells, *Annu. Rev. Immunol.* 36 (2018) 489–517.

- [32] Y. Zhou, M. Fei, G. Zhang, W.C. Liang, W. Lin, Y. Wu, R. Piskol, J. Ridgway, E. McNamara, H. Huang, J. Zhang, J. Oh, J.M. Patel, D. Jakubiak, J. Lau, B. Blackwood, D.D. Bravo, Y. Shi, J. Wang, H.M. Hu, W.P. Lee, R. Jesudason, D. Sangaraju, Z. Modrusan, K.R. Anderson, S. Warming, M. Roose-Girma, M. Yan, Blockade of the phagocytic receptor MerTK on tumor-associated macrophages enhances P2X7R-dependent STING activation by tumor-derived cGAMP, *Immunity* 52 (2020) 357–373.e359.
- [33] J. Ahn, T. Xia, A. Rabasa Capote, D. Betancourt, G.N. Barber, Extrinsic phagocyte-dependent STING signaling dictates the immunogenicity of dying cells, *Cancer Cell* 33 (2018) 862–873.e865.
- [34] K. McArthur, L.W. Whitehead, J.M. Heddleston, L. Li, B.S. Padman, V. Oorschot, N. D. Geoghegan, S. Chappaz, S. Davidson, H. San Chin, R.M. Lane, M. Dramicanin, T. L. Saunders, C. Sugiana, R. Lessene, L.D. Osellame, T.L. Chew, G. Dewson, M. Lazarou, G. Ramm, G. Lessene, M.T. Ryan, K.L. Rogers, M.F. van Delft, B.T. Kile, BAK/BAX Macropores Facilitate Mitochondrial Herniation and mtDNA Efflux during Apoptosis, *Science*, New York, N.Y., 2018, p. 359.
- [35] M.J. White, K. McArthur, D. Metcalf, R.M. Lane, J.C. Cambier, M.J. Herold, M. F. van Delft, S. Bedoui, G. Lessene, M.E. Ritchie, D.C. Huang, B.T. Kile, Apoptotic caspases suppress mtDNA-induced STING-mediated type I IFN production, *Cell* 159 (2014) 1549–1562.
- [36] D.B. Doroshow, S. Bhalla, M.B. Beasley, L.M. Sholl, K.M. Kerr, S. Gnijatic, Wistuba II, D.L. Rimm, M.S. Tsao, F.R. Hirsch, PD-L1 as a biomarker of response to immune-checkpoint inhibitors, *Nature reviews, Clin. Oncol.* 18 (2021) 345–362.
- [37] P.C. Tumeh, C.L. Harview, J.H. Yearley, I.P. Shintaku, E.J. Taylor, L. Robert, B. Chmielowski, M. Spasic, G. Henry, V. Ciobanu, A.N. West, M. Carmona, C. Kivork, E. Seja, G. Cherry, A.J. Gutierrez, T.R. Grogan, C. Mateus, G. Tomasic, J. A. Glaspy, R.O. Emerson, H. Robins, R.H. Pierce, D.A. Elashoff, C. Robert, A. Ribas, PD-1 blockade induces responses by inhibiting adaptive immune resistance, *Nature* 515 (2014) 568–571.
- [38] S. Eisinger, D. Sarhan, V.F. Boura, I. Ibarluceta-Benitez, S. Tyystjärvi, G. Oliynyk, M. Arsenian-Henriksson, D. Lane, S.L. Wikström, R. Kiessling, T. Virgilio, S. F. Gonzalez, D. Kaczynska, S. Kanatani, E. Daskalaki, C.E. Wheelock, S. Sedimbi, B. J. Chambers, J.V. Ravetch, M.C.I. Karlsson, Targeting a scavenger receptor on tumor-associated macrophages activates tumor cell killing by natural killer cells, *Proc. Natl. Acad. Sci. U.S.A.* 117 (2020) 32005–32016.
- [39] H.M. Lazear, J.W. Schoggins, M.S. Diamond, Shared and distinct functions of type I and type III interferons, *Immunity* 50 (2019) 907–923.
- [40] E.C. Borden, Interferons α and β in cancer: therapeutic opportunities from new insights, *Nature reviews, Drug discovery* 18 (2019) 219–234.
- [41] R. Yu, B. Zhu, D. Chen, Type I interferon-mediated tumor immunity and its role in immunotherapy, *Cellular and molecular life sciences, CMLS* 79 (2022) 191.
- [42] S.R. Woo, M.B. Fuertes, L. Corrales, S. Spranger, M.J. Furdyna, M.Y. Leung, R. Duggan, Y. Wang, G.N. Barber, K.A. Fitzgerald, M.L. Alegre, T.F. Gajewski, STING-dependent cytosolic DNA sensing mediates innate immune recognition of immunogenic tumors, *Immunity* 41 (2014) 830–842.
- [43] J. Wu, L. Sun, X. Chen, F. Du, H. Shi, C. Chen, Z.J. Chen, Cyclic GMP-AMP is an endogenous second messenger in innate immune signaling by cytosolic DNA, *Science (New York, N.Y.)* 339 (2013) 826–830.
- [44] L. Schadt, C. Sparano, N.A. Schweiger, K. Silina, V. Cecconi, G. Lucchiari, H. Yagita, E. Guggisberg, S. Saba, Z. Nascaova, W. Barchet, M. van den Broek, Cancer-cell-intrinsic cGAS expression mediates tumor immunogenicity, *Cell Rep.* 29 (2019) 1236–1248.e1237.
- [45] A. Marcus, A.J. Mao, M. Lensink-Vasan, L. Wang, R.E. Vance, D.H. Raulet, Tumor-derived cGAMP triggers a STING-mediated interferon response in non-tumor cells to activate the NK cell response, *Immunity* 49 (2018) 754–763.e754.

Abbreviation

Tumor-associated macrophages: (TAMs)
 hepatocellular carcinoma: (HCC)
 programmed cell death protein-1: (PD-1)
 program cell death protein ligand-1: (PD-L1)
 collagen-like structure macrophage receptor: (MARCO)
 immunohistochemistry: (IHC)
 bone marrow-derived macrophages: (BMDM)
 overexpressed MARCO: (OE-MARCO)
 Cyclic GMP-AMP synthase: (cGAS)
 cyclic guanosine monophosphate–adenosine monophosphate: (cGAMP)
 stimulator of interferon genes: (STING)